

Electrochemical oxidation of benzyl germatranes

S. Soualmi^a, L. Ignatovich^b, E. Lukevics^b, A. Ourari^a, V. Jouikov^{c,*}

^a *Laboratory of Electrochemistry, Molecular Engineering and Redox Catalysis, University of Setif, 19000 Setif, Algeria*

^b *Institute of Organic Synthesis, Latvian Academy of Sciences, LV-1006 Riga, Latvia*

^c *UMR 6510 SESO, University of Rennes I, 35042 Rennes, France*

Received 5 December 2007; received in revised form 16 January 2008; accepted 17 January 2008

Available online 26 January 2008

Abstract

The electrooxidation of ring-substituted bromobenzylgermatranes in CH₃CN and DMF solutions was studied. By cyclic voltammetry supported by DFT B3LYP/6-311G calculations, donor activity of the nitrogen atom was shown to be substantially reduced because of the dative N → Ge coordination compared to Et₃N and (HOCH₂CH₂)₃N. In the electrochemical context, the transmission of electronic effects between the ArCH₂ moiety and the reaction center (the lone pair of N pointed inside the atrane cage) is well described by the generalized additive inductive model including mesomeric interactions. The oxidation process follows classical scheme for tertiary amines – reversible electron transfer with the ensuing deprotonation of α-carbon atom; at low scan rates the process is reversible/quasi-reversible and at higher rates it is under electron transfer control. Anodic cyanation of *m*-bromobenzylgermatrane was performed.

© 2008 Elsevier B.V. All rights reserved.

Keywords: Cyclic voltammetry; Electrooxidation; Germatranes; Silatranes; Electron transfer

1. Introduction

Germatranes, germanium derivatives of the atrane family, are tricyclic compounds with an intramolecular penta-coordination of Ge which show a large palette of rich and various biological activities. Due to their unique physico-chemical and biological properties, these compounds attract keen attention of researchers; several reviews cover their synthesis, reactivity and biological properties [1–5]. Driven by the interest for germatranes, a remarkable effort in their synthetic chemistry was accomplished [6–11]. Chemical structure, molecular modeling and theoretical studies of these compounds [12–16] at different levels of theory, including correlated post-Hartree–Fock methods [16] allowed better understanding of the specificity of *trans*-annular N → Ge bond and revealed the importance of interaction of Ge with all 5 substituents [13–15]. Biological activity of germatranes that is closely bound with the

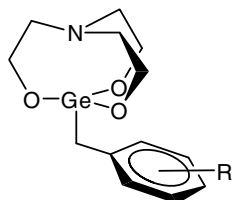
substitution character at Ge was extensively studied [1,4–6,17,18]. On the other side, the redox properties of germatranes, which are often playing an important role in biological activity, are considerably less explored. Meanwhile silicon homologues of germatranes, silatranes, were shown to possess interesting redox activity [19]. Silatrane moiety, acting as substituent, exhibits electron-donor properties [20] as witnessed by the decrease of the redox potential of silatrane-substituted ferrocene, whereas own oxidation of the silatranes is more difficult compared to triethylamine and other tertiary amines [21] picturing the lack of electron density on the lone pair of N that acts as reaction center of electron transfer during the oxidation. Detailed study on electrooxidation of silatranes was reported [22,23] but electrochemistry of germanium derivatives has not been studied so far and only the oxidation potentials of three germatranes: methyl-, 3-furyl- and 3-thienylgermatrane have been reported [23].

In the present communication, we describe the results of the anodic oxidation of four recently prepared benzyl germatranes **1–4** [9] showing high neurotropic activity,

* Corresponding author. Tel.: +33 223236293.

E-mail address: vjouikov@univ-rennes1.fr (V. Jouikov).

the study undertaken in order to elucidate their redox properties, the role of intramolecular N → Ge coordinating interactions in their electrochemical reactivity and an attempt to use electrochemistry for the functionalization of these compounds.



- 1 R = H
 2 R = *o*-Br
 3 R = *m*-Br
 4 R = *p*-Br

2. Experimental

2.1. Instrumentation

Voltammetric and chronoamperometric experiments were performed using a PAR 2273 and a EG&G Model 362 scanning potentiostats. Glassy carbon discs of 0.7 and 3 mm diameter or a 0.5 mm Pt disc were used as working electrode and, for this purpose, carefully polished before each run. The counter electrode was a glassy carbon rod and the reference electrode was Ag/0.1 M AgNO₃ in CH₃CN, separated from the solution by an electrolytic bridge filled with CH₃CN/0.1 M Bu₄NPF₆. DMF and CH₃CN containing 0.1 M Bu₄NPF₆ or Bu₄NBF₄ were used as supporting electrolytes. IR-compensation facility of the potentiostat was always used to account for ohmic drops in the solution. To correct the experimental potentials, voltammograms of ferrocene were traced under similar conditions and $E_{(\text{Fc}^+/\text{Fc})}^0 = 0.158$ vs. SCE was used as the reference. Unless otherwise stated, the temperature was controlled at 20 °C.

The electrolyses have been performed under the inert atmosphere in a 15 mL coaxial three-electrode three-compartment electrochemical cell, with a 15 × 2 × 30 mm glassy carbon plate as working electrode.

2.2. Reagents and solutions

Syntheses of germatranes [9] and of vinylsilatran [22] were described previously. Analytical grade CH₃CN (sds) and DMF (Acros) were twice distilled under Ar atmosphere from CaH₂ and BaO, respectively. Electrochemical grade tetrabutylammonium hexafluorophosphate, tetrafluoroborate (Fluka) and cyanide (Aldrich) were dried in a desiccator over P₂O₅ and used without further purification.

Product of cyanation of vinylsilatran, **5a** (65% yield). ¹H NMR (CDCl₃, TMS), δ ppm: 5.78–6.00 (3H, vinyl), 3.90 (d, 2H, CH₂-O_{CN}, *J* = 6.9 Hz), 3.83 (t, 4H, CH₂-O), 2.87

(t, 4H, CH₂-N), 2.43 (t, H, CH-CN, *J* = 6.9 Hz); ¹³C (CDCl₃): 139.65, 129.49 (vinyl), 119.52 (CN), 62.58 (C-O), 55.84, 52.65 (C-N); LC-MS (CI): 227 (M+H)⁺.

Product of cyanation of **3** (47% NMR yield). ¹H NMR (CDCl₃, TMS), δ ppm: 7.73 (s, 1H, *o*-Br), 6.68, 6.90, 7.43 (3H, Ar), 3.67 (d, 2H, CH₂-O_{CN}, *J* = 11.4 Hz), 3.3–3.45 (4H, CH₂-O), 2.66 (t, H, CH-CN, *J* = 11.4 Hz), 2.47 (4H, CH₂-N), 2.10 (s, 2H, CH₂-Ge); ¹³C (CDCl₃): 136.52, 132.40, 132.01, 130.37, 125.47 (Ar), 114.53 (CN), 58.76 (C-O), 55.92 (C-N), 48.95 (CH₂-Ge).

3. Results and discussion

Anodic oxidation of benzyl germatranes **1–4** and of the model compounds – vinylsilatran (**5**), triethylamine (**6**) and triethanolamine (**7**) was studied in CH₃CN and DMF solutions. Upon oxidation in 0.1 M Bu₄NPF₆ solution in these solvents, all four germatranes show a distinct peak (Fig. 1) whose reproducibility depends on the compound and varies with the solvent and the electrode material. In general, the voltammograms obtained at glassy carbon (GC) electrode are in most cases better than those at Pt. Currents are better reproducible in DMF, probably because the basicity of germatranes is lower in this solvent and the adsorptional interactions with the electrode are weaker. There is also a second oxidation signal at about $E_p \cong 2 \dots 2.1$ V (Fig. 1), observed only in CH₃CN, which is much less reproducible and is usually seen as a whole only in the first scan. This peak is tentatively attributed to the ensuing oxidation of the primary cation radicals. Peak currents i_p for **1–4** are linear with the concentration and, for $v > 0.5$ –1 V s⁻¹, with the square root of the scan rate ($i_p/v^{1/2} = \text{const.}$, Fig. 2), thus suggesting diffusional control of the process.

The electron stoichiometry for the first step of oxidation (Table 1) in all cases was determined either from direct comparison of the limiting currents of the germatranes and ferrocene, taking no account the difference in their diffusion coefficients *D*, or combining voltammetry parameter $i_p/v^{1/2}$ with the Cottrell slope obtained from chronoampe-

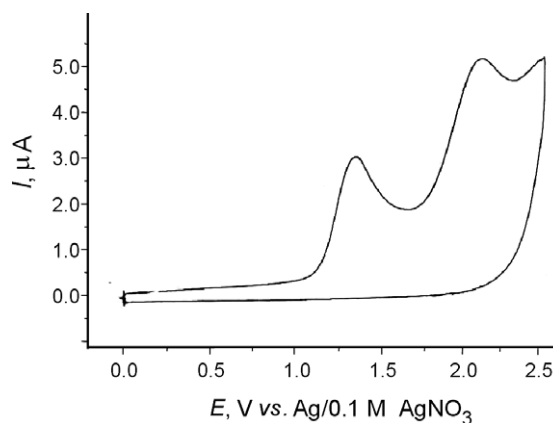


Fig. 1. Cyclic voltammogram of **3** ($C = 2 \text{ mmol L}^{-1}$) in CH₃CN/0.1 M Bu₄NPF₆ at a 0.7 mm glassy carbon electrode. $v = 10 \text{ V s}^{-1}$; $T = 22 \text{ }^\circ\text{C}$.

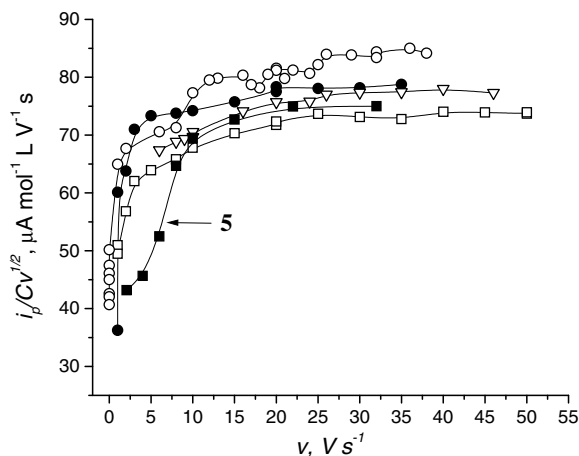


Fig. 2. Normalized oxidation peak currents $i_p C^{-1}v^{-1/2}$ of: (○) – 1; (●) – 2; (▽) – 3; (□) – 4; (■) – 5. GC disc electrode, $\text{CH}_3\text{CN}/0.1 \text{ M Bu}_4\text{NPF}_6$.

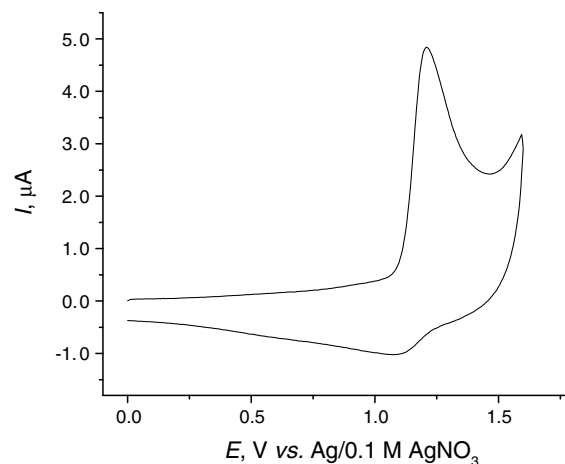


Fig. 3. Cyclic voltammogram of **1** ($C = 0.8 \text{ mmol L}^{-1}$) in $\text{CH}_3\text{CN}/0.1 \text{ M Bu}_4\text{NPF}_6$ at a 0.7 mm GC electrode. $v = 32 \text{ V s}^{-1}$; $T = 22 \text{ }^\circ\text{C}$.

rometry at the same electrode and the same solution [24]. Beyond the lowest scan rates ($v \geq 0.2\text{--}0.5 \text{ V s}^{-1}$) both methods provide the n value close to 1.

At higher scan rates, a reverse peak appears on the voltammograms of the non-substituted **1** and, to a lesser extent, of *p*-Br benzylgermatrane (**4**) (Fig. 3). Though the oxidation peaks of both compounds are the narrowest in the reaction series ($E_p - E_{p/2}$ in Table 1), the $E_p^a - E_p^c$ difference (118 and 110 mV for **1** and **4**, respectively) for these peaks is somewhat too large to correspond to a perfectly reversible redox couple so the process can rather be characterized as a quasi-reversible one.

Compared to silatranes [23], the compounds **1–4** show less reversible voltammograms: only small cathodic signal appears for **1** (Fig. 3) at $v \cong 30 \text{ V s}^{-1}$, which does not grow upon further increasing the scan rate. Instead, the $\Delta E_p / \Delta \lg(v)$ slope, that tends to 30 mV at lower scan rates, increases at $v \cong 30\text{--}250 \text{ V s}^{-1}$ as electron transfer kinetics becomes the limiting step.

Though chemical grafting to the electrode during the oxidation of tertiary amines is usually not observed [25] and the germatranes are supposedly even less prone to it because of the involvement of the lone pair of nitrogen into

the dative intramolecular N \rightarrow Ge bonding, the surface of the electrode showed a remarkable trend to passivate, especially in CH_3CN . On this reason, it was hard to cover a large span of concentrations for the oxidation of **1–4** to study their $E_p - \lg(C)$ behavior: at $C > 2 \times 10^{-3} \text{ mol L}^{-1}$ the adsorption starts deforming the shape of the voltammograms. However, a careful examination of E_p of **1** in the interval of concentrations $5 \times 10^{-4} \leq C \leq 2 \times 10^{-3} \text{ mol L}^{-1}$ with the increment of $2.5 \times 10^{-4} \text{ mol L}^{-1}$ does not show any visible dependence of E_p on C thus ruling out bimolecular self-reactions of electrogenerated cation radicals [26]. This is also in agreement with the slopes of linear $E_p - \lg(v)$ dependence for **1–4** at $v < 10\text{--}20 \text{ V s}^{-1}$ (Table 1).

At $v < 0.1 \text{ V s}^{-1}$, the normalized oxidation peak current $i_p/v^{1/2}$ decreases (Fig. 2) instead of expected increasing due to the growing contribution of the spherical diffusional flow. Using larger electrodes in order to respect the semi-infinite diffusion conditions at low scan rates, the n value was shown to tend to 0.5 at $v \rightarrow 0$ thus corresponding to the case of hidden limiting currents of third type (reaction of electrochemically produced species with the starting molecule [27]). This fact might reflect a slow protonation

Table 1
Parameters of anodic oxidation of germatranes **1–4** and of the model compounds at a GC disc electrode

Cmpd	E_p (V) ^a		$E_p - E_{p/2}$ (V)		$\Delta E_p / \Delta \lg(v)$ (mV)		n	E^o (V)	k_s^b	α^c	IP (eV)	σ^{*d}
	CH_3CN	DMF	CH_3CN	DMF	CH_3CN	DMF						
1	1.209		59		37		1.1	1.149	11.1	0.80	6.016	1.526
2	1.285		101		45		1.0	1.237	4.1	0.57	6.238	1.994
3	1.276		109		39		1.0	1.225	2.0	0.60	6.225	1.703
4	1.236	1.364	83	74	33	34	0.9	1.202	4.4	0.74	6.105	1.660
5	0.774	0.795	169	124	36	41	1.0					
6	0.582	0.888	193	145	64		0.9					
7	1.126		497		98		0.9					

^a Peak potential at $v = 1 \text{ V s}^{-1}$ vs. Ag/0.1 M AgNO_3 in CH_3CN .

^b $k_s \times 10^2$ in cm s^{-1} .

^c Transfer coefficient estimated as a mean of α from $\Delta E_p / \Delta \lg(v) = 29.6/\alpha$ and $E_p - E_{p/2} = 1.85 \text{ RT}/\alpha F$ [38].

^d Group inductive constants calculated according to Eq. (1) [33].

of the starting germatrane by protons arising from the deprotonation of its cation radicals. A similar electron stoichiometry was observed during large-scale electrooxidation of tertiary amines [25].

In fact, being oxidized under similar conditions, tertiary amines **6** and **7** – the nearest non-cyclic models without Ge – exhibit similar signals and behavior but at less anodic potentials (Table 1, Fig. 4).

In **6** and **7**, as is reflected by the trend in E_p (Table 1), the basicity of nitrogen is higher than in germatranes because of N → Ge interaction in the latter, so the protonation rate of **1–4** is slower. Also, slightly higher oxidation potentials of the germatranes versus E_p of silatranes [23] indicate larger involvement of the lone pair of N in N → Ge relative to N → Si dative interaction; consequently, this site is less available for oxidation and protonation. Indeed, the same behavior of i_p was observed for **5** but as expected from its basicity, at higher scan rates (Fig. 2). When a strong proton donor, CF₃COOH, was added to the solution of **1**, no oxidation signal was observed confirming that the lone pair of nitrogen atom loses its electron donating properties. The same happens when free protons, eliminated from the cation radical, protonate a non-oxidized germatrane.

Vinylsilatrane (**5**) shows the same number of transferred electrons and essentially similar anodic behavior as **1–4**, indicating that the Ge atom does not bring any dramatic changes to the electrochemical reactivity of the atranes family. Therefore, primary steps of the electrooxidation of **1–4** are similar to those of silatranes (EC mechanism) which is in general typical for tertiary amines in the absence of nucleophiles: reversible electron transfer followed by deprotonation of the cation radical.

The E_p of few known germatranes, are 70–100 mV higher than the E_p of homologous silatranes [23]. For benzylsilatrane, the oxidation potential is not known. Nevertheless, its value was estimated as $E_p \cong 1.45$ V vs. SCE (1.12 V

vs. Ag/Ag⁺) using the $\rho\sigma$ -equation, provided in Ref. [23] for the oxidation potentials of various organosilatranes, and the σ Taft constant for the PhCH₂ group [28]. This value is about 90 mV less anodic compared to E_p of **1**.

The oxidation potentials of **1–4** also show a distinct dependence on the substitution at the aromatic ring of benzyl. With this, the analysis of the electrochemical reactivity of **1–4** in terms of the effect of substitution in the phenyl ring is not a straightforward task for several reasons. First, there are no substituent constants available specifically for this type of reaction center; second, the reaction series **1–4** is not large enough to provide high statistical validity of $\rho\sigma$ -correlations. Nevertheless, as far as is seen from this limited series, the E_p of **1–4** – though showing a physically sound trend, – do not correlate neither with solely Taft nor Hammett constants. Indeed, contrary to the Taft's model, the methylene group at Ge in benzylgermatranes does not cut off all non-inductive interactions because of a different mechanism of transmission of electronic effects (Fig. 5).

On the other hand, as was pointed out in Ref. [23], the E_p of silatranes with the substituents whose interaction with the reaction center is more complex than purely inductive, do not obey Taft's correlation. Indeed, for **1–4** B3LYP/6-311G molecular modeling (see below) revealed at least one additional feature ruled by stereoelectronic effects. The fact that the optimized ground-state equilibrium structures not only of **1**, **3** and **4** but also of the *ortho*-derivative **2** all show the configuration where two O atoms are eclipsed with the carbons at *o*-,*o'*-positions of benzene ring (which in general provides about 2–5 kcal/mol gain in energy compared to the non-eclipsed configuration), suggests the existence of additional *trans*-annular electronic interactions between Ge and the aromatic moiety, transmitted by oxygen atoms. These interactions are seen in somewhat more positive potential E_p of **2** (*ortho*) where the eclipsed configuration is partially distorted.

An additional point is that there is no unifying approach to describe the reactivity of organoelement compounds using the classical “carbon” scale. Various “silicon” (σ_{Si}) and other scales are known [29]. Furthermore, the importance of polarizability effect, – the ion-dipole interaction of the partial charge on N atom with the dipole that it induced on the Si(Ge)–R bond, – was pointed out in Refs. [30–32]. The analysis of known E_p of silatranes with including the σ_x polarizability constants in the correlation has shown this effect to contribute up to 17% in the shift of E_p [30]. To provide some solution, a two-parameter model taking into account both inductive and mesomeric effects was therefore considered. Trying Taft and similar constants [28] for this correlation, it was found that better adequacy with the experimental data was achieved using unified the inductive constants σ^* (Table 1) based on the additive model of inductive effect, developed by Cherkasov et al. [33] and corrected to the “Ge-scale”

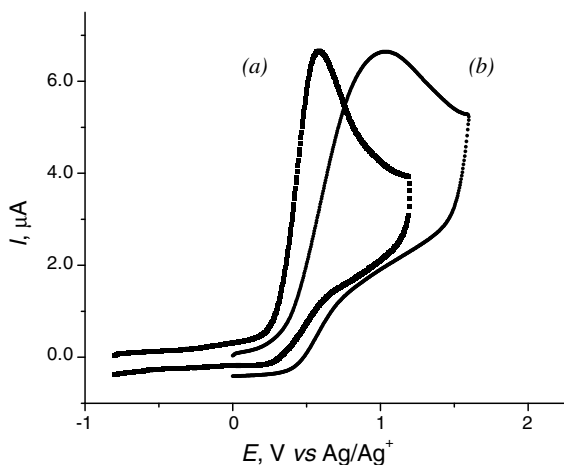


Fig. 4. Cyclic voltammograms of oxidation of (a) **6** and (b) **7** ($C = 1$ mmol L⁻¹) in CH₃CN/0.1 M Bu₄NPF₆ at a 0.7 mm glassy carbon electrode. $v = 35$ V s⁻¹.

$$\sigma^* = 7.84 \Sigma \{ \Delta \chi_i (R_i/r_i)^2 \} \quad (1)$$

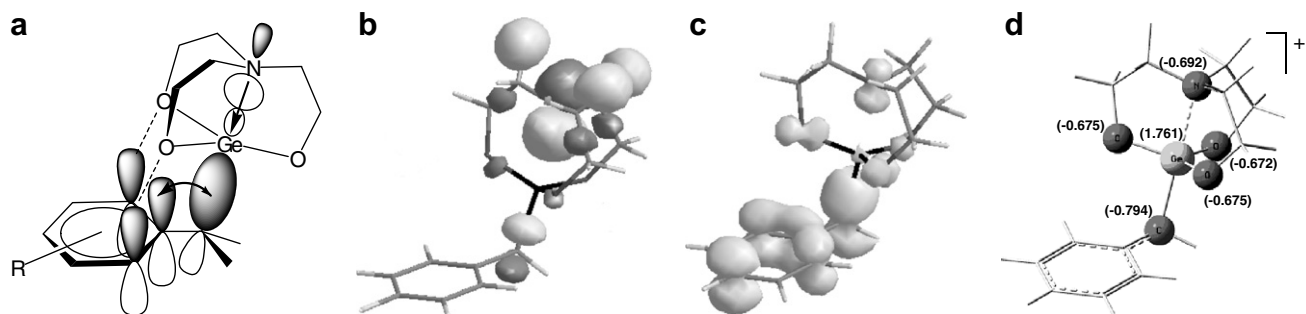


Fig. 5. From left to right: (a) stereoelectronic interactions in **1–4** affecting their oxidation potentials E_p ; (b) HOMO of **1**; (c) spin density (SOMO) in 1^+ ; (d) geometry and Mulliken charge distribution in 1^+ according to B3LYP/6-311G calculations.

here $\Delta\chi_i$ is the difference of electronegativities [34] between i th atom and the reaction center; R_i is the i th atom covalent radius and r_i is its distance from the reaction center. Geometrical parameters were taken from [28] and from the geometries optimized by B3LYP/6-311G calculations, respectively. As the second set, the Hammett constants [28] were used to account for non-inductive interactions. There resulted the following two-parameter correlation:

$$E_p = E_p^H + \rho^+ \sigma^+ + \rho^* \sigma^* = 1.209 + 0.11\sigma^+ + 0.016\sigma^* \quad (2)$$

ρ^* and ρ^+ are inductive and mesomeric reaction constants, correlation coefficient $R = 0.995$. This multiparameter model, though made on a limited data, provided best description of the electrochemical reactivity of benzylgermatranes. It is noteworthy that the inductive reaction constant ρ^* is positive, reflecting acceptor interactions of benzyl with the reaction center, which agrees with the electronegativities of the atoms concerned. With the inductive constants calculated in the hypothesis that N is the immediate reaction center, ρ^* is expected to be negative. The same is true for silatranes, so this model also agrees with the electron-donor character of silatrane moiety, pointed out in Ref. [20].

It is interesting that the ionization potentials IP of **1–4**, calculated by B3LYP/6-311G (as $-\varepsilon_{\text{HOMO}}$ in Koopman's approach) follow the same row as their E_p . The IP – E_p correlation¹ forms a straight line with no deviation that might be caused by the kinetic contribution. This fact can be interpreted as that the kinetic shift of E_p versus E° due to the deprotonation of cation radicals is either absent or is practically constant within the reaction series, or at least it does not exceed the uncertainty of such rough consideration.

The analysis of the electrochemical reactivity was seconded with *ab initio* molecular modeling. To account for specific interactions of Ge with its neighborhood, it is reasonable to use basis sets not lower than 6-31G, so the geometry optimization and frequency analysis of **1–4** were performed by DFT B3LYP/6-311G method using TITAN program [37]. As was pointed out in Ref. [15], the “soft-

ness” of N–M (M = Si, Ge) coordinate accounts for the difference in its length when determined by different methods. In methylsilatrane, e.g., the N–Si distance measured by X-ray diffractometry is shorter than that obtained from B3LYP/6-31G* and MP2/6-31G* calculations. The same trend was observed for **1–4**: the N–Ge interatomic distance, obtained by B3LYP/6-311G, is systematically 10–12% longer than those found by X-ray crystallographic analysis of these compounds [9]. The HOMO of **1–4**, mostly corresponding to the n -electrons of N atom (Fig. 5), is far higher compared to the next lower-lying occupied orbital, HOMO–1 (built with the important contribution of the orbitals of benzyl fragment, $\Delta\varepsilon_{\text{HOMO} - (\text{HOMO}-1)} \cong 0.3\text{--}0.8\text{ eV}$), therefore electron withdrawal during the electro-oxidation (Table 1) unambiguously occurs at this site. Meanwhile, the nitrogen atom in the cation radical of **1** does not carry any remarkable part of spin neither charge density: spin density is almost entirely localized on the benzyl fragment and the positive charge is mostly carried by Ge (Fig. 5). Due to this positive charge, *trans*-annular N → Ge interaction is enhanced compared to the neutral molecule; as a consequence, the N–Ge distance in 1^+ is shortened (Table 2). In general, the configuration around Ge atom in 1^+ is much closer to a trigonal bipyramid than in **1**: three $\angle\text{O–Ge–C}$ angles are closer to 90° , the difference between Ge–N and Ge–C(H₂) distances is smaller (Table 2); in addition, the configuration of the methylene carbon of benzyl is closer to C_{sp^3} reflecting the charge-induced contraction of the structure of 1^+ .

These results corroborate well the observed quasi-reversible character of the oxidation of **1–4**. Complex electron density re-distribution occurs during the redox transformation: $1 - e \rightleftharpoons 1^+$; the reaction centers of forward and reverse processes – oxidation of **1** and of reduction of 1^+ back to **1** – are not the same since related to different atoms and orbitals.

If the positive charge in the cation radical was not transferred to Ge and remained on N, as in simple tertiary amines, its electrostatic repulsion with Ge (carrying a partial δ^+ charge due to the three acceptor O-atoms) would favor *exo*-form of 1^+ over *endo*- 1^+ . However, the comparison of these conformers by B3LYP/6-311G has shown the *endo*-form to be $\cong 6.96\text{ kcal mol}^{-1}$ more stable than

¹ The base for separation of complex reaction constants is given in Refs. [35,36].

Table 2
Selected geometrical parameters of **1** and **4** and of their cation radicals (B3LYP/6-311G)

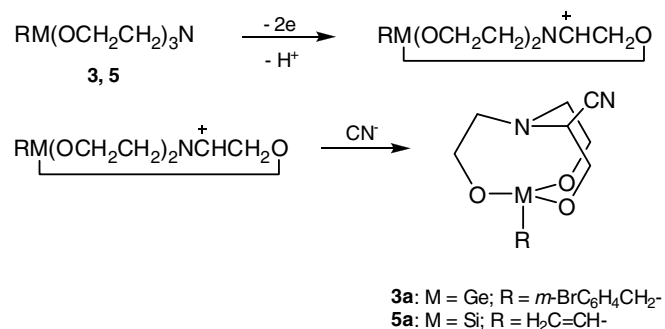
	$L(\text{N}-\text{Ge})$ (Å)	$l(\text{Ge}-\text{CH}_2)$ (Å)	$l(\text{Ge}-\text{C}_{\text{Ph}}^1)$ (Å)	av. $l(\text{Ge}-\text{O})$ (Å)	av. $\angle\text{CH}_2-\text{Ge}-\text{O}$ (°)	$\angle\text{Ge}-\text{CH}_2-\text{C}_{\text{Ph}}^1$
1	2.527	1.958	2.931	1.819	102.8	114.8
1 ⁺	2.208	2.104	2.905	1.811	95.4	108.8
4	2.516	1.923	2.881	1.774	104.3	113.9
4 ⁺	2.148	2.072	2.859	1.768	95.9	108.8

exo-**1**⁺. Solvation in polar CH₃CN would evidently modify this value but the trend must be the same. The change of entropy, $\Delta S(\mathbf{1} \rightarrow \mathbf{1}^+)$, obtained from harmonic frequency analysis, only amounts to $-0.6 \text{ kcal K}^{-1} \text{ mol}^{-1}$ showing that neither symmetry nor the number of vibrations change upon oxidation. Therefore, the decreased electron transfer rate during the oxidation of **1–4** is related to rather solvent reorganization accompanying charge redistribution in the cation radical (Connolly solvent accessible areas for **1** and **1**⁺ are similar) than to a slow flip-flopping of N between *exo*- and *endo*-configurations.

Under the electron transfer control, observed for **1–4** at $v > 30\text{--}250 \text{ V s}^{-1}$, the oxidation potentials E_p depend on three fundamental parameters: E° , k_s and α . Using transfer coefficient α values (Table 1), obtained by two methods, the standard potential E° and the electron transfer rate constant k_s were determined by iteratively solving $E_p = f(E^\circ, k_s, \alpha, v)$ equations [38]. The obtained values are collected in Table 1. Non-substituted benzylgermatran (**1**) has highest k_s value which agrees with the partial reversibility, observed for this compound. On the other hand, at $v < 30 \text{ V s}^{-1}$ the electron transfer is not yet the rate limiting step and the oxidation of **1** follows a EC scheme. Under these conditions, knowing the E° and using Eq. (3) [26], it was possible to determine the rate of the fast deprotonation of **1**⁺. Thus obtained constant is rather high: $k = 3.98 \times 10^3 \text{ s}^{-1}$. For Br-substituted benzylgermatranes **2–4**, electron-withdrawing substitution increases the positive charge in the cation radical rendering its α -protons more acid and therefore increasing its deprotonation rate. As a result, the oxidation of **2–4** is under a mixed-kinetic and electron transfer-control.

$$E_p = E^\circ + (RT/F)[0.738 - 0.5 \ln(kRT/vF)] \quad (3)$$

Deprotonation of α -carbon in the cation radicals of atranes was used to effect the oxidative functionalization of **3** and **5** by anodic substitution. For that, 1.5 mmol of the corresponding atrane was oxidized at a GC anode under anhydrous and methanol-free conditions slightly modified compared to those described in Refs. [39,40]: in CH₃CN containing 0.1 M Bu₄NCN as supporting salt and the source of CN⁻ anion and in a three-compartment cell. The electrolyses were carried out at the controlled potentials of $E = 1.2 \text{ V}$ **3** and 0.8 V **5** until ca. 1.5–1.8 F/mol of electricity were passed and resulted in α -cyanated germatran (**3a**) and silatran (**5a**), respectively. Some amounts of unreacted atranes were also recovered.



The exact mechanism of anodic cyanation being in general complex [26], one can suppose the process to occur according to the simplified scheme above.

4. Conclusions

The electrochemical behavior, the oxidation mechanism, the results of the electrolysis and DFT calculations show that the reaction center of the oxidation of the germatranes studied is localized on N atom: though substantially pointed inside towards Ge and thus hidden in the atrane cage, and affected by stereoelectronic interactions with the orbitals of C–C, Ge–C σ -bonds and O atoms, it is still the n -electrons of nitrogen that bring the main contribution to the HOMO of these compounds.

Though from the results of mass spectroscopy investigation of germatranes with various substituents at Ge it has been concluded that *trans*-annular effect N \rightarrow Ge is insignificant [41], the oxidation potentials of **1–4**, the $E_p^a - E_p^c$ difference and the character of interaction of the substituent at Ge with the reaction center on one hand, and the DFT calculations on the cation radical **1**⁺ on the other show the importance of N \rightarrow Ge interactions in the reactivity of these compounds. It perfectly agrees with the results of electrooxidation of substituted silatranes [22,23] and $\approx 8\text{--}20 \text{ kcal mol}^{-1}$ experimental values for the N \rightarrow Si interaction in silatranes reported by Voronkov [42,43].

Once formed, the cation radicals of germatranes exist in *endo*-conformation, the geometry around Ge atom being closer to trigonal bipyramid than in the neutral molecule. Slow electron transfer and fast deprotonation limit observing the cation radicals of germatranes but on the other side allow the anodic substitution reactions at the α -carbon atom, driving force of the process being the deprotonation of this site. This reaction was used to achieve α -cyanation

of *m*-bromobenzyl germatrane and of vinylsilatrane, the process that might provide a convenient means for the functionalization of this type of compounds.

References

- [1] E. Lukevics, L.M. Ignatovich, in: S. Patai (Ed.), *The Chemistry of Organic Germanium, Tin and Lead Compounds*, John Wiley & Sons Ltd., 1995, pp. 857–863.
- [2] E.A. Chernyshev, S.P. Knyazev, V.N. Kirin, V.G. Lakhtin, *Russ. Khim. Zhurn.* 42 (1998) 120–125.
- [3] S.S. Karlov, G.S. Zaitseva, *Chem. Heterocyclic Comp. (New York)* 37 (2001) 1325–1357.
- [4] E. Lukevics, L. Ignatovich, in: Z. Rappoport (Ed.), *The Chemistry of Organic Germanium, Tin and Lead Compounds*, vol. 2, John Wiley & Sons Ltd., Chichester, 2002, pp. 1653–1683.
- [5] E. Lukevics, L. Ignatovich, in: M. Gielen, E.R.T. Tiekink (Eds.), *Metallotherapeutic drugs and metal-based diagnostic agents, The Use of Metals in Medicine*, John Wiley & Sons Ltd., Chichester, 2005, pp. 278–295.
- [6] E. Lukevics, S. Germane, L. Ignatovich, *Appl. Organomet. Chem.* 6 (1992) 543–564.
- [7] L. Ignatovich, S. Belyakov, J. Popelis, E. Lukevics, *Chem. Heterocyclic Comp. (New York)* 36 (2000) 603–606.
- [8] S.S. Karlov, P.L. Shutov, A.V. Churakov, J. Lorberth, G.S. Zaitseva, *J. Organomet. Chem.* 627 (2001) 1–5.
- [9] E. Lukevics, L. Ignatovich, T. Shul'ga, O. Mitchenko, S. Belyakov, *J. Organomet. Chem.* 659 (2002) 165–171.
- [10] J.W. Faller, R.G. Kultyshev, J. Parr, *J. Organomet. Chem.* 689 (2004) 2565–2570.
- [11] E. Lukevics, L. Ignatovich, T. Shul'ga, S. Belyakov, *Appl. Organomet. Chem.* 19 (2005) 167–168.
- [12] E. Lukevics, L. Ignatovich, S. Belyakov, *Chem. Heterocyclic Comp. (New York)* 43 (2007) 243–249.
- [13] I.S. Ignatyev, T.R. Sundius, D.V. Vrazhnov, T.A. Kochina, M.G. Voronkov, *J. Organomet. Chem.* 692 (2007) 5697–5700.
- [14] M.V. Zabalov, S.S. Karlov, G.S. Zaitseva, D.A. Lemenovskii, *Russ. Chem. Bull.* 55 (2006) 464–476.
- [15] E.A. Chernyshev, S.P. Knyazev, V.N. Kirin, I.M. Vasilev, N.V. Alekseev, *Russ. J. Gen. Chem.* 74 (2004) 58–65.
- [16] A.A. Milov, R.M. Minyaev, V.I. Minkin, *Russ. J. Org. Chem.* 39 (2003) 340–347.
- [17] J. Satge, G. Rima, M. Fatome, H. Sentenac-Roumanou, C. Lion, *Eur. J. Med. Chem.* 24 (1989) 48–54.
- [18] L. Ignatovich, S. Belyakov, Yu. Popelis, E. Lukevics, *Chem. Heterocyclic Comp. (New York)* 36 (2000) 603–606.
- [19] K.G. Solymos, B. Varhegyi, E. Kalman, F.H. Karman, M. Gal, P. Hencsei, L. Bihatsi, *Corr. Sci.* 35 (1993) 1455–1462.
- [20] G. Cerveau, C. Chuit, E. Colomer, R.J.P. Corriu, C. Reye, *Organometallics* 9 (1990) 2415–2417.
- [21] K. Broka, V.T. Glezer, J. Stradins, in: *Proceedings of the 41st Meeting of ISE, Prague, Czechoslovakia, 20–25 August 1990*, Th-14.
- [22] K. Broka, V.T. Glezer, J. Stradins, G. Zelcans, *Zhurn. Obshch. Khim.* 61 (1991) 1374–1378.
- [23] K. Broka, J. Stradins, V. Glezer, G. Zelcans, E. Lukevics, *J. Electroanal. Chem.* 351 (1993) 199–206.
- [24] P. Malachuk, *Anal. Chem.* 41 (1969) 1493–1494.
- [25] A. Adenier, M.M. Chehini, I. Gallardo, J. Pinson, N. Vila, *Langmuir* 20 (2004) 8243–8253.
- [26] H. Lund, O. Hammerich (Eds.), *Organic Electrochemistry*, 4th ed., Marcel Dekker Inc., NY, 2001.
- [27] J. Heyrovsky, J. Kuta, *Principles of Polarography*, Mir, Moscow, 1965, 560p.
- [28] A.J. Gordon, R.A. Ford, *The Chemist's Companion*, Wiley Interscience, John Wiley & Sons, NY, 1972.
- [29] L.T. Kanerva, A.M. Klibanov, *J. Am. Chem. Soc.* 111 (1989) 6864.
- [30] M.G. Voronkov, A.N. Egorochkin, O.V. Kuznetsova, *J. Organomet. Chem.* 691 (2006) 159–164.
- [31] O.V. Novikova, O.V. Kuznetsova, A.N. Egorochkin, M.G. Voronkov, *Abstr. IV European Silicon Days, Bath, 9–11 September 2007*.
- [32] A.N. Egorochkin, M.G. Voronkov, O.V. Kuznetsova, O.V. Novikova, *J. Organomet. Chem.* 693 (2007) 181–188.
- [33] R.A. Cherkasov, V.I. Galkin, R.A. Cherkasov, *Russ. Chem. Rev.* 65 (1996) 641–656.
- [34] D.R. Lide (Ed.), *CRC Handbook of Chemistry and Physics*, 75th ed., The Chem. Rubber Co., Cleveland, London, 1994, pp. 9–51.
- [35] P. Zuman, *Substituent Effects in Organic Polarography*, Plenum Press, New York, 1967, 384p.
- [36] Y.M. Kargin, V.Z. Latypova, O.G. Yakovleva, *Russ. J. Org. Chem.* 50 (1980) 2327–2332.
- [37] M.D. Beachy, Y. Cao, R.B. Murphy, J.K. Perry, W.T. Pollard, M.N. Ringnald, G.R. Vacek, J.R. Wright, B.J. Deppmeier, A.J. Driessen, W.J. Hehre, J.A. Johnson, P.E. Klunzinger, M. Watanabe, J. Yu, TITAN release 1.07. Wavefunction Inc., Schrodinger Inc., 1999–2003.
- [38] C.P. Andrieux, J.M. Saveant, in: C.F. Bernasconi (Ed.), *Investigations of Rates and Mechanisms of Reactions*, Wiley, New York, 1986 (Chapter VII).
- [39] A. Konno, T. Fuchigami, Y. Fujita, T. Nonaka, *J. Org. Chem.* 55 (1990) 1952–1954.
- [40] H.J. Callot, A. Louati, M. Gross, *Tetrahedron Lett.* 21 (1980) 3281–3284.
- [41] A.E. Chernyshev, V.N. Bochkarev, *Zhurn. Obshch. Khim.* 57 (1987) 154–157.
- [42] M.G. Voronkov, V.P. Baryshok, V.A. Klyuchnikov, A.N. Korzhagina, V.I. Pepekin, *J. Organomet. Chem.* 359 (1989) 167–169.
- [43] E.I. Brodskaya, M.G. Voronkov, *Izv. Akad. Nauk SSSR, Ser. Khim.* (1986) 1694.